J. Fluid Mech. (1990), *vol.* 211, *pp.* 595–608
Printed in Great Britain

Nonlinear flow phenomena in a symmetric sudden expansion

R. M. FEARN[1], T. MULLIN[1] AND K. A. CLIFFE[2]

[1] Clarendon Laboratory, Parks Road, Oxford OX1 3PU, UK

[2] Theoretical Physics Division, Harwell Laboratory, Didcot, Oxfordshire OX11 0RA, UK

(Received 29 March 1989 and in revised form 29 July 1989)

The origin of steady asymmetric flows in a symmetric sudden expansion is studied using experimental and numerical techniques. We show that the asymmetry arises at a symmetry-breaking bifurcation and good agreement between the experiments and numerical calculations is obtained. At higher Reynolds numbers the flow becomes time-dependent and there is experimental evidence that this is associated with three-dimensional effects.

1. Introduction

In recent years significant progress has been made in the ability to calculate and measure fluid behaviour in a variety of physical systems. In particular, the application of ideas from bifurcation theory to multiple solutions of nonlinear hydrodyanmic problems, has led to a clearer understanding of observed events and their role in the field of hydrodynamic stability and transition to turbulence (see for example Drazin & Reid 1982).

Taylor–Couette flow has become a very useful vehicle for testing and developing these ideas, since it has proved possible to compare exacting experimental data with the results obtained from numerical analysis. In certain cases the transition from laminar to turbulent flow seems to arise through a complex sequence of mechanisms that have their roots in steady symmetry-breaking bifurcation phenomena (see for example Mullin & Cliffe 1986). We show below that a similar type of steady bifurcation is the first instability encountered as the Reynolds number is increased.

In this paper we apply the ideas and manner of investigation that has proved so successful in understanding flow phenomena in the Taylor–Couette closed system, to an open-system channel flow problem. We describe a thorough experimental and numerical study of the fundamental flow phenomena in a plane, sudden, symmetric and nominally two-dimensional channel expansion. This geometry was chosen because previous observations of the flow in such a channel, had shown the existence of flows which were asymmetric about the central plane of the channel (see Durst, Melling & Whitelaw 1974). It is well known that an initial symmetric flow becomes asymmetric with respect to this line of symmetry, as the Reynolds number, Re, is increased. This is sometimes referred to as the 'Coanda' effect in the literature.

The present work is the first extensive application of bifurcation ideas to an experimental investigation of the flow in a plane symmetric expansion. However, Cliffe & Greenfield (1982) and Sobey & Drazin (1986) have used these ideas to perform numerical studies of the flow in smoothed, symmetric, two-dimensional channel expansion. Cliffe & Greenfield used a finite-element approximation to the

governing two-dimensional Navier–Stokes equations and Sobey & Drazin used a finite-difference method for their calculations. In both cases flows that were asymmetric with respect to the channel centreline were shown to arise via a symmetry-breaking bifurcation. The numerical results of Sobey & Drazin, however, gave a bifurcation diagram with a more complicated structure than that of Cliffe & Greenfield, including additional solution multiplicity and hysteresis. Recently, Fuchs (1988) used a finite-difference approximation to solve the discrete two-dimensional Navier–Stokes equations, describing the flow in a plane, symmetric expansion, using a multi-grid procedure. His results also predicted the occurrence of a symmetry-breaking bifurcation.

Experimental observations of flows through a symmetric channel expansion are given by Durst *et al.* (1974), Cherdron, Durst & Whitelaw (1978), John (1984) and Sobey (1985). The main results show that the initial flow, with recirculation regions behind each step and symmetrically displaced with respect to the channel centreline, becomes unstable at a Reynolds number that depends on the expansion ratio and aspect ratio of the channel. The width of the channel is thus constant over the working section of the flow rig, and the height increases by a factor of three. Above that Reynolds number a pair of steady asymmetric flows are observed as one recirculation region grows at the expense of the other. As Re is increased further, various events may occur according to the channel configuration. The flow may become first three-dimensional and then time-dependent or vice versa. Ultimately the flow becomes turbulent as Re increases further. Studies by Abbott & Kline (1962) and Restivo & Whitelaw (1978) have shown that flow asymmetry and hence solution multiplicity remains a feature of flows in the turbulent regime.

The experimental measurements were performed on a specially designed flow rig using laser-Doppler velocimetry and flow visualization techniques. The experimental arrangement is described in §2. Flow features were studied in a single channel of expansion ratio 3:1 and downstream aspect ratio 8:1. Here the aspect ratio is defined to be the width to height ratio of the channel. Thus the sequence of events is studied by variation of a single controlling parameter, the Reynolds number, defined by

$$Re = \frac{dU}{\nu},$$

where d is the upstream channel half-height, U the maximum inlet velocity and ν the kinematic viscosity.

In §3 we make a direct comparison of experimental and numerical results in the Reynolds number regime close to the onset of flow asymmetry. The numerical solutions were calculated using nonlinear bifurcation methods on the CRAY2 at Harwell Laboratory.

In §4 we extend the study to high Reynolds numbers to investigate the occurrence of further steady flows, and to discuss the importance and the nature of time-dependent and three-dimensional effects. Calculations are performed to determine whether the transition to time-dependence occurs via a two-dimensional Hopf bifurcation or by some other means.

Finally in §5 we make concluding remarks on the implications of the reported results.

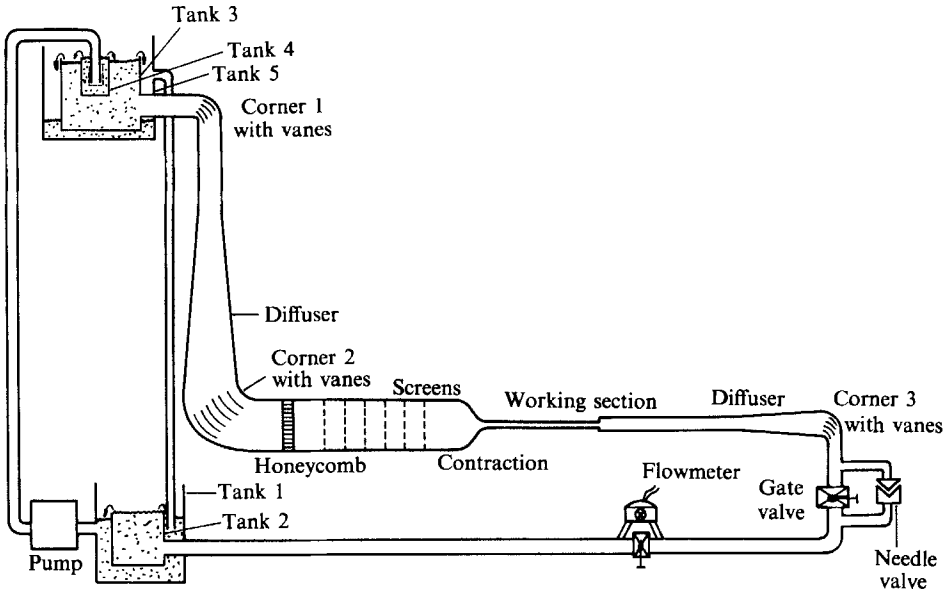

FIGURE 1. Schematic diagram of the flow rig. The overall length of the system is ~ 2 m and the height of the upper flow tank is ~ 3.5 m above the base.

2. Experimental arrangement

The flow-rig used for the experimental study is shown schematically in figure 1. Care was needed in the flow-rig design to ensure accurate control of the incoming flow within the channel and of the single variable parameter, Re, over the whole range of study.

The flow channel was operated as a continuous flow circuit, so as to allow flow oscillations and time-dependence, first observed by Durst *et al.* (1974), enough time to develop and be studied in full. The flow was driven by a constant-head tank through a series of flow-conditioning units within the channel. These conditioning units included diffusers, corner vanes, a honeycomb, screens and a contraction and were inserted within the channel to suppress any spatial and temporal non-uniformity of the flow. Details of the particular specifications of each unit, implemented in the channel, may be found in Fearn (1988). The flow conditioners provided steady well-controlled flow immediately upstream of the working section for a Reynolds number range 0–400. These conditioning units preceded a long entry section, 60 channel-heights long, that provided sufficient length for the required parabolic entry profile to develop fully. A two-dimensional flow profile was achieved upstream of the expansion by an entry section of aspect ratio 24:1. The fluid then flowed through a 1:3 symmetric, plane expansion into a section 80 step-heights in length and of aspect ratio 8:1. Work by Cherdron *et al.* (1978) had shown that the low Reynolds number flow was nominally two-dimensional in a channel with such an aspect ratio. Downstream of the working section the flow was conditioned further by means of a diffuser and corner vanes so that the flow at the expansion was not significantly affected by upstream influences. The fluid then entered a lower storage tank, from which it was returned to the upper tank by means of a pump. The pump was isolated from the circuit by a series of tanks and meshes that minimized any unsteadiness introduced by it.

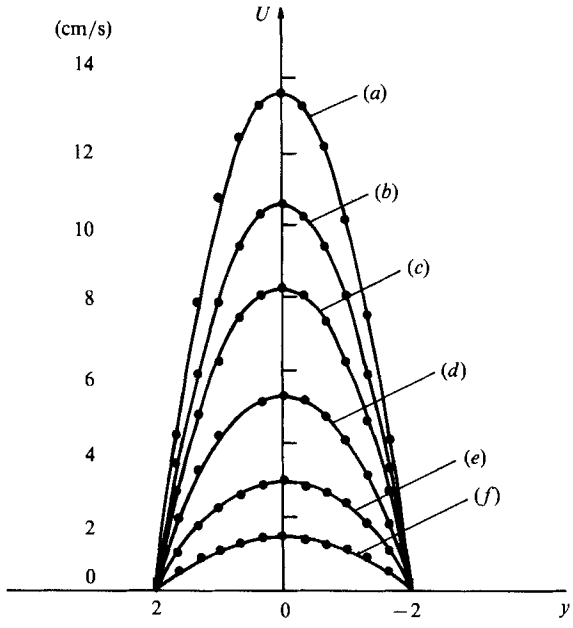

FIGURE 2. Experimental variation of the inlet velocity profile with Re, $x = -15$ mm. The continuous curves show parabolic profiles at (*a*) $Re = 273$, (*b*) 210, (*c*) 164, (*d*) 106, (*e*) 59 and (*f*) 29; the points indicate corresponding experimental measurements.

The fluids used were water glycerol mixtures with kinematic viscosities of approximately 7 cSt for studies in the Reynolds-number range up to $Re = 60$. For higher Reynolds number investigations, up to $Re = 380$, distilled water was used. Accurate control of the flow to approximately 1 % in Reynolds number was achieved by frequent measurement of fluid viscosity, careful construction of the flow rig and sensitive velocity control, using a gate valve for coarse adjustment and a bypass needle valve for fine adjustment.

The flow features were studied using laser-Doppler velocimetry (LDV) and flow visualization techniques to accurately identify the values of the control parameter Re at which changes in the flow type occurred. The laser system was operated in the differential Doppler, forward-scatter mode. Equal intensity beams from a 5mW helium-neon laser were employed to measure either the longitudinal or the vertical component of fluid velocity in the channel. Light was scattered by small latex spheres introduced into the working fluid to achieve a good quality signal. The resultant signal was processed by a TSI counter-type processing unit, whose output was an analogue voltage proportional to the flow velocity. For time-dependent flows, the sampled voltage signal was fed to a MASSCOMP computer for further processing to provide time series and power spectra of the oscillations. The whole optical system was mounted in a linear traverse that enabled manual movement in a longitudinal direction and computer-controlled automatic movement in a vertical direction. The optical system could thus be moved without becoming misaligned and exact repeatability of measurement position could be achieved. In addition computer-controlled velocity profiles of the flow both upstream and downstream of the expansion could be recorded by scanning the channel vertically.

A qualitative analysis of the flow features was made using flow visualization

techniques. Light-reflecting Mearlmaid A.A. particles, mixed into the fluid, were illuminated by a thin sheet of light in the vertical midplane of the channel. Photographs of the flow features were also taken using Ilford XP1 film ratio at ASA 1000. This allowed for typical exposure time of 1–2 s.

The nature of the inlet flow achieved, using this experimental arrangement, is shown as a series of velocity profiles in figure 2. Profiles at Reynolds numbers from 30 to 280 were recorded at a position 15 mm upstream of the expansion in the vertical centreplane of the channel. Experimental points corresponding to values on each measured profile are compared in the figure with parabolas. We conclude from figure 2 that, to within experimental error, the flow at the expansion had the fully developed parabolic profile form required by the investigation.

3. The symmetry-breaking bifurcation

In this section we present the experimental results obtained using the techniques described in §2. In all cases the experimental results are compared with the results of a numerical calculation performed on the CRAY2 at Harwell Laboratory. The calculations were performed using numerical bifurcation techniques applied to a finite-element discretization of the two-dimensional Navier–Stokes equations. Details of the basic numerical methods will not be given here since they have been covered elsewhere (Cliffe 1989). The application of the techniques to study flow in this geometry is described in Fearn (1988). Calculations of the flows were carried out using a grid of rectangular elements that covered the working section, and which was locally refined near to the expansion. The calculations of the symmetric flows and symmetry-breaking bifurcation points were performed using techniques to exploit the symmetry so that only half the domain was discretized. Asymmetric flows and limit points were calculated on the full grid. The results were checked for accuracy by refining the mesh and repeating the calculations. The overall accuracy of the numerical results was thus determined to be better than 0.2%. In addition it was found that the results were unchanged as the length of either the inlet or the outlet section was doubled.

An initial qualitative analysis using flow visualization techniques showed that at Reynolds numbers less than approximately 35 there is a unique stable flow at each value of Reynolds number. This flow possessed a reflectional symmetry about the midplane of the channel, with two identical regions of recirculating flow behind the steps of the expansion. Such a flow with a Reynolds number of 25 is shown in figure 3(*a*). A visualization of the experimental flow can be compared with the corresponding numerical streamline plot of figure 3(*b*). The two figures can be seen to have strong similarities.

A futher quantitative comparison of numerical and experimental flows in this regime is provided by the series of velocity profiles shown in figure 4, at a Reynolds number of 26. Points on the experimentally produced profiles are plotted on top of the calculated profiles as a function of distance in step-heights, h, downstream of the expansion. At all four measurement stations the profiles remain symmetric about their centrelines to within the experimental error and good agreement can be seen between experimental and numerical results. At stations corresponding to downstream distances $1.25h$ and $2.5h$, flow reversal within the recirculation regions is readily identifiable. The result at distance $10h$ downstream of the expansion shows that the flow profile is once again parabolic

As the Reynolds number was increased to values above 33, no stable flow with this

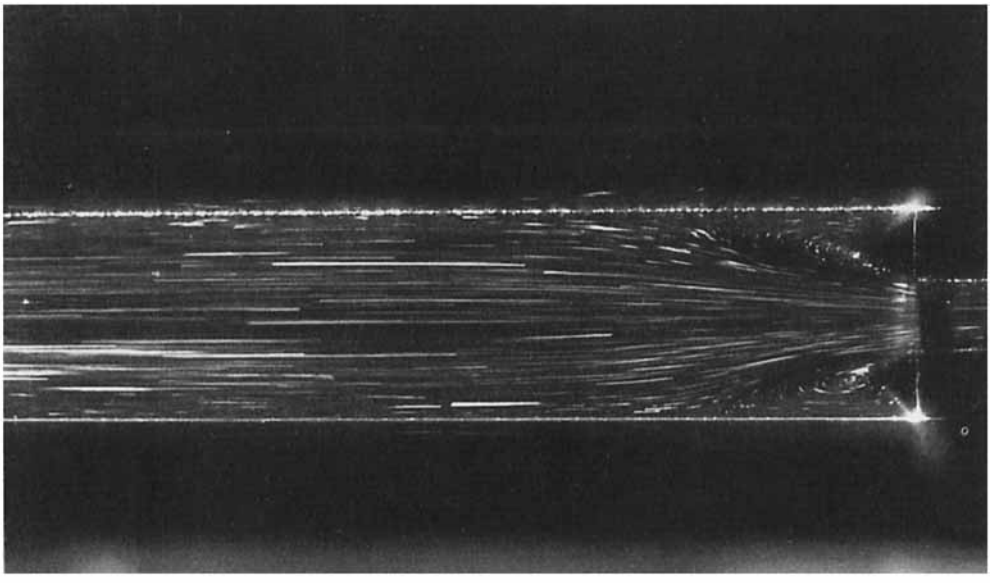

(a)

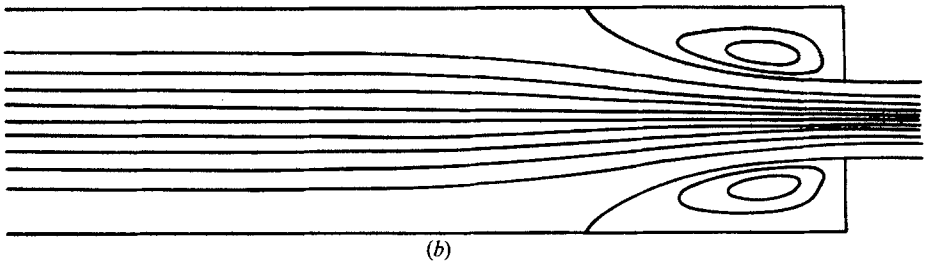

(b)

FIGURE 3. (a) Flow visualization at $Re = 25$. (b) Calculated streamlines at $Re = 25$.

configuration could be found. Instead the symmetric flow lost stability to one of a pair of steady asymmetric solutions with either the upper or lower circulation region becoming longer. An asymmetric pair of solutions in this regime at $Re = 80$ are shown in figures 5(a) and 6. Figure 5(b) shows the corresponding streamline plot from the numerical calculations and displays good agreement with the corresponding experimental flow, figure 5(a).

Good agreement between experimental and numerical results of flow in this steady asymmetric regime is also shown in the series of velocity profiles presented in figure 7. The results at $Re = 60$ indicate that the flow retains a marked asymmetry, until it becomes parabolic once more at a downstream distance of $20h$.

This exchange of stability between symmetric and asymmetric flows is seen in more detail in the bifurcation diagram of figure 8. In the figure, the normalized vertical velocity of the flow at a point 25.5 mm downstream of the expansion on the centreline of the channel is used as a sensitive measure of the flow asymmetry. In the

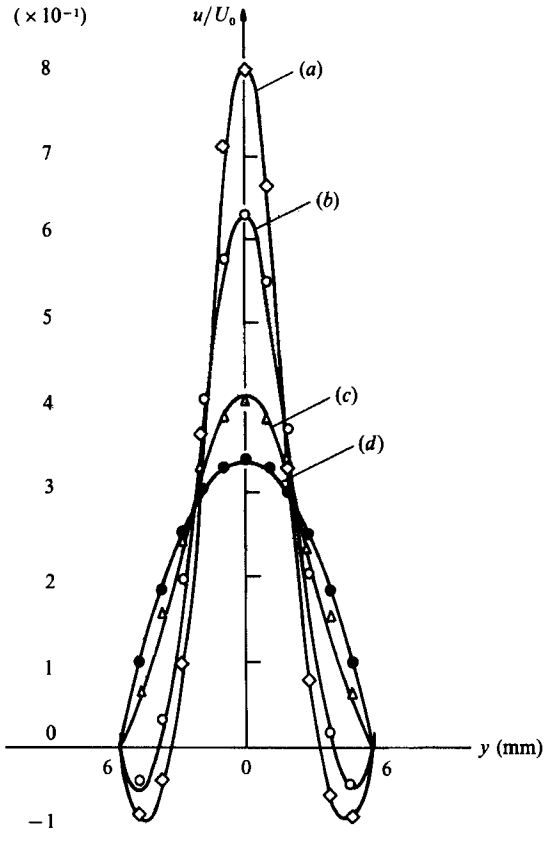

FIGURE 4. Numerical and experimental velocity profiles at $Re = 26$. The numerically calculated profiles are shown as continuous curves. (*a*) ◇, $x/h = 1.25$; (*b*) ○, $x/h = 2.5$; (*c*) △, $x/h = 5$; (*d*) ●, $x/h = 10$.

symmetric flow regime the vertical component is zero and becomes non-zero as the flow becomes asymmetric, with a sign that initially depends on the sense of the asymmetry. The accurate LDV measurements allowed changes of 0.01 cm (a 1% change at $Re = 44$) to be identified.

The figure compares the measured experimental data, representing the average of a series of measurements at each value of Re, with the calculated numerical bifurcation diagram for flow in a perfectly symmetrical channel.

The numerical results predict that the unique stable solution to the steady two-dimensional Navier–Stokes equation loses stability at a critical value of Reynolds number of $Re_c = 40.45 \pm 0.17\%$, via a symmetry-breaking bifurcation. Above this value of Re_c, the equations have three solutions, of which the original solution is now unstable. As a consequence of the symmetry in the geometry of the problem, the two stable solutions above Re_c are a pair of asymmetric solutions of opposite senses with respect to the line of symmetry.

Away from the immediate vicinity of the bifurcation point, the experimentally measured degree of asymmetry at each value of Re shows a satisfactory agreement with the corresponding value obtained from the numerical results. Both asymmetric solution branches are apparent and the flow does indeed seem to have undergone a symmetry-breaking bifurcation. The experimental bifurcation diagram is however

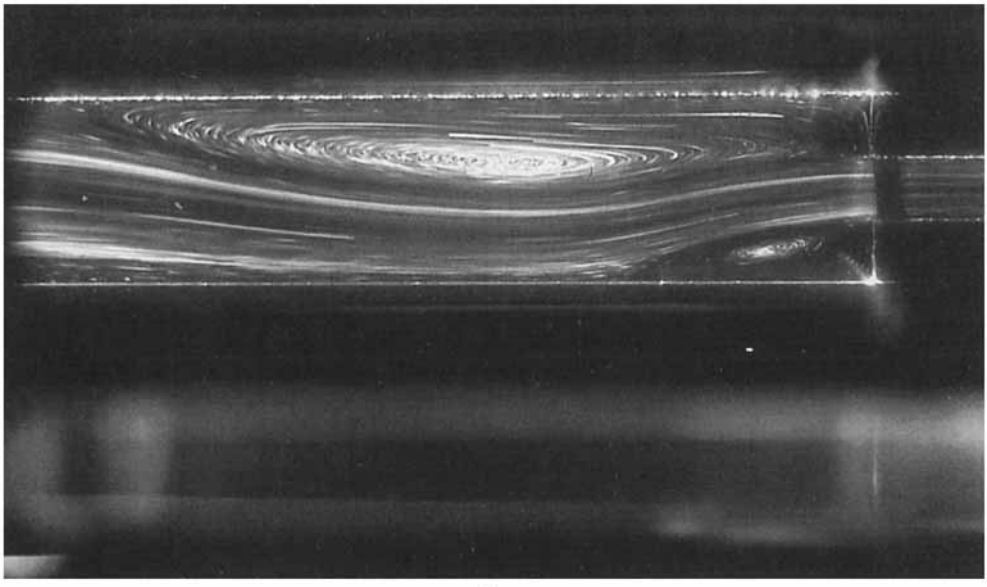

(a)

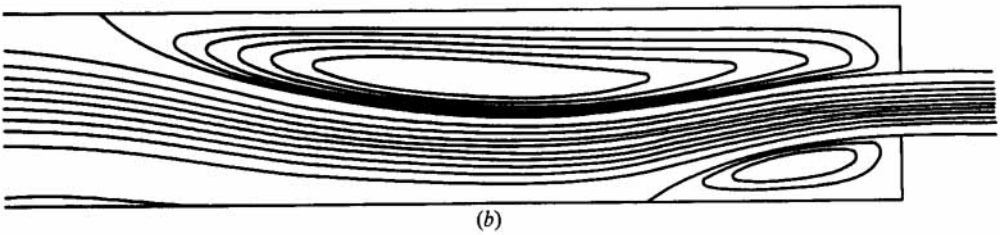

(b)

FIGURE 5. (a) Flow visualization at $Re = 80$. (b) Calculated streamlines at $Re = 80$.

disconnected, owing to small imperfections that are inevitably present in the experimental apparatus. There was thus no experimentally observed critical value of Reynolds number and, therefore, no perfectly symmetric state; i.e. v/U_0 asymptotes to zero as Re tends to zero. Instead only the upper branch of the bifurcation diagram could be reached by continuous increase of Re, corresponding to a flow with a longer upper circulation. The lower branch, corresponding to a flow with a longer lower circulation region, was disconnected and could only be reached by starting the flow impulsively at $Re > 50$. By this method, it was found that the larger separation might attach to either side of the channel without preference. The low-Reynolds-number limit of stability on the lower branch, was found, by decreasing Re, to occur at $Re = 47.3$. The flow then lost stability catastrophically to a flow corresponding to a point on the upper branch.

An attempt was made to model numerically the effect of small imperfections in the flow channel, in order to try to account for the disconnection in the experimental bifurcation diagram. The calculations were repeated when the whole downstream section of the grid was shifted up by 0.05 mm with respect to the axis of symmetry.

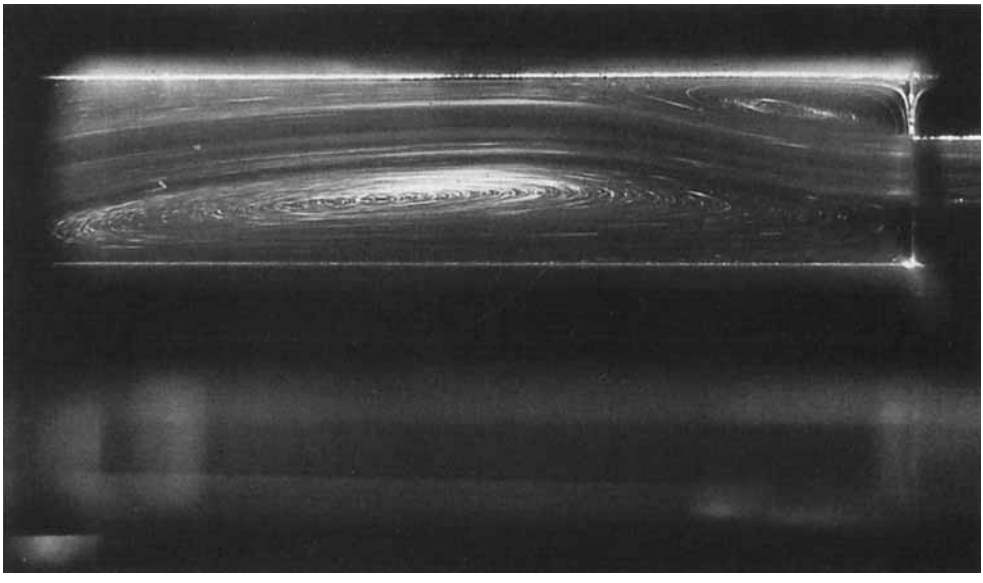

FIGURE 6. Inverted solution of the asymmetric pair at $Re = 80$.

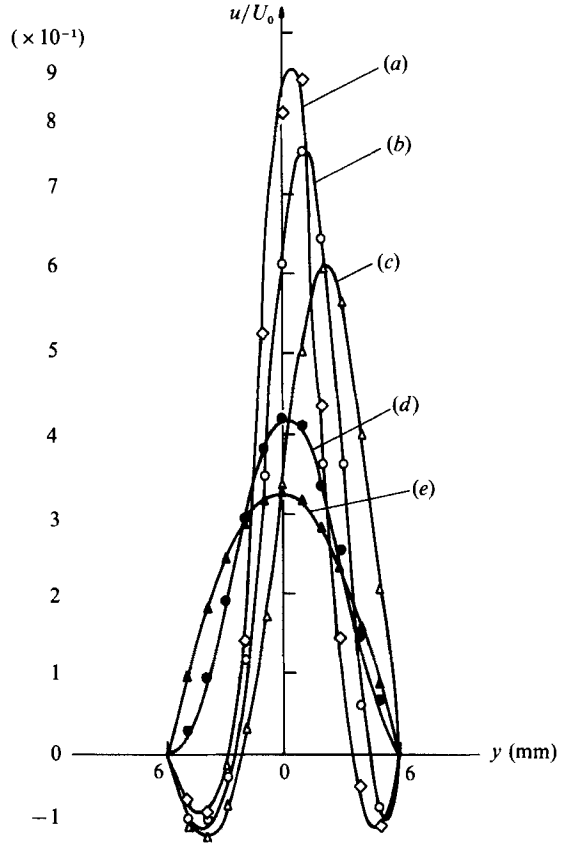

FIGURE 7. Numerical and experimental profiles $Re = 60$. The numerically calculated profiles are shown as continuous curves. (*a*) ◇, $x/h = 1.25$; (*b*) ○, $x/h = 2.5$; (*c*) △, $x/h = 5$; (*d*) ●, $x/h = 10$; (*e*) △, $x/h = 20$.

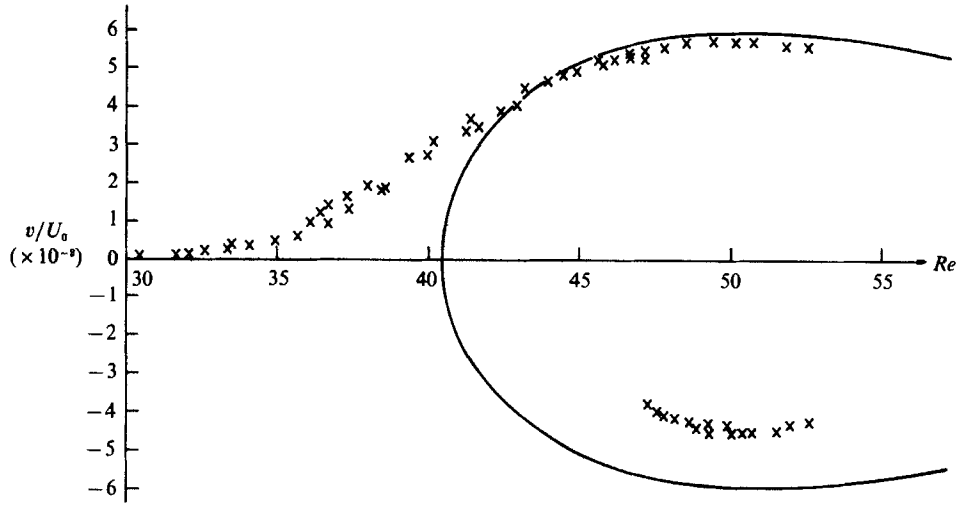

FIGURE 8. Experimental and numerical bifurcation diagram. The vertical component of velocity at the middle of the channel cross-section 25.5 mm from the expansion is plotted against the Reynolds number.

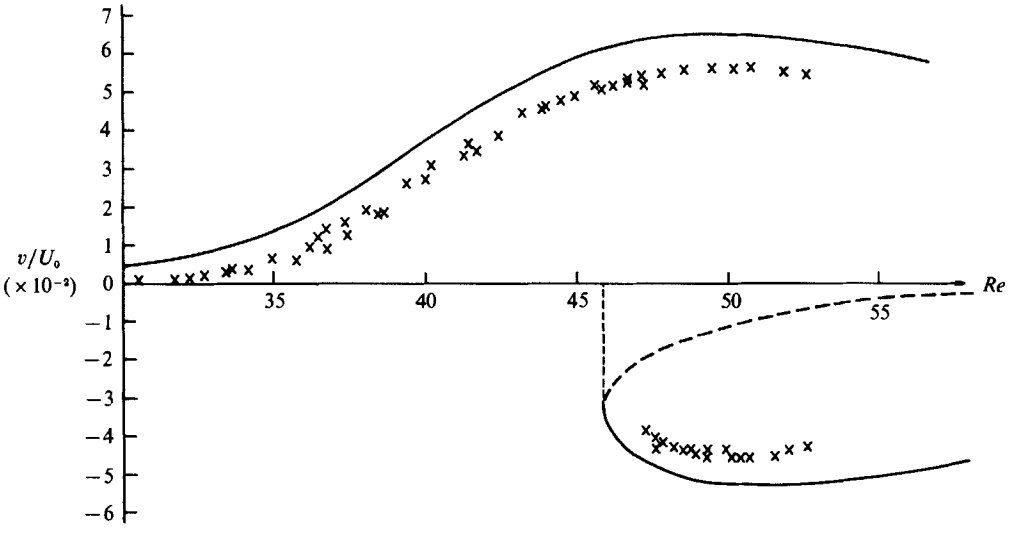

FIGURE 9. As for figure 8 except that the numerical results are for the perturbed grid.

This perturbation corresponds to less than a 1% change in the apparatus and represents the estimated imperfection in the alignment of the two sections. The effect of this small pertubation is shown, in figure 9, to disconnect the bifurcation diagram and cause a shift in the limit point of over 13% from the original critical point. The experimental data, included on the figure, show that the size of the disconnection found experimentally is of the same order as the size of the decoupling produced by perturbing the numerical problem. The main features of the flow recorded are, thus, fundamental properties of the Navier–Stokes equations and not features of the accuracy of this particular experimental arrangement.

It is interesting to note, however, that the effect of the imperfection in this open

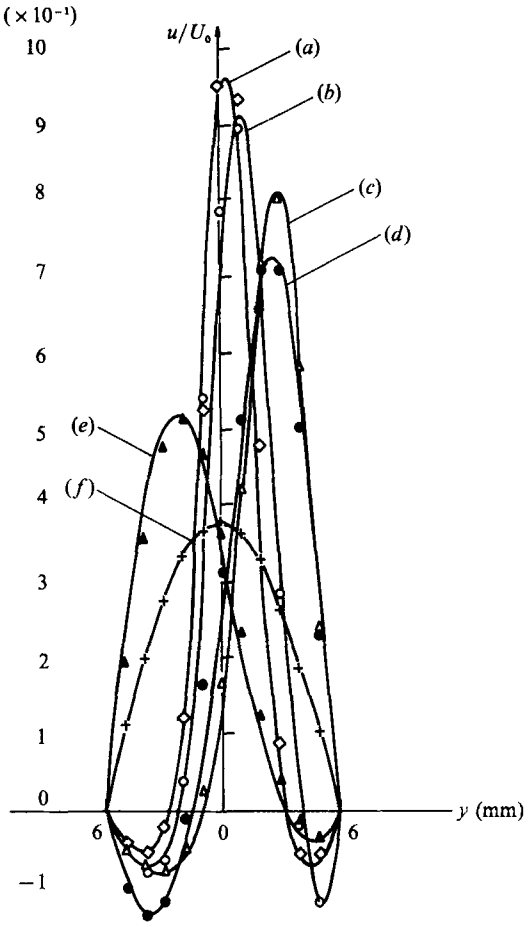

FIGURE 10. Numerical and experimental velocity plots at $Re = 140$. The numerically calculated profiles are shown as continuous curves. (*a*) ◇, $x/h = 1.25$; (*b*) ○, $x/h = 2.5$; (*c*) △, $x/h = 5$; (*d*) ●, $x/h = 10$; (*e*) △, $x/h = 20$; (*f*) +, $x/h = 40$.

system seems to be much greater than in a closed one, such as the Taylor–Couette system, where the disconnection is only of the order 1–2% (see Pfister *et al.* 1988).

4. Higher Reynolds number effects

The investigation was extended to higher values of Re in order to study the development of the flow beyond the initial symmetry-breaking bifurcation.

At a Reynolds number of 125 a third recirculation region was observed opposite the downstream end of the large separation region and on the same wall as the initial small recirculation. Calculations performed on the numerical model showed that this third separation region is a feature of the solution to the steady two-dimensional Navier–Stokes equations. Evidence of this third separation region is given in figure 10 which compares numerical and experimental velocity profiles at $Re = 140$. Flow reversal is observed close to the lower wall ($y = -6$), in figure 10(*e*), at a distance 20 h downstream of the expansion, but not in the two preceding stations upstream (figures 10*c* and 10*d*). The figure demonstrates the close agreement between

FIGURE 11. Calculated streamlines at $Re = 140$.

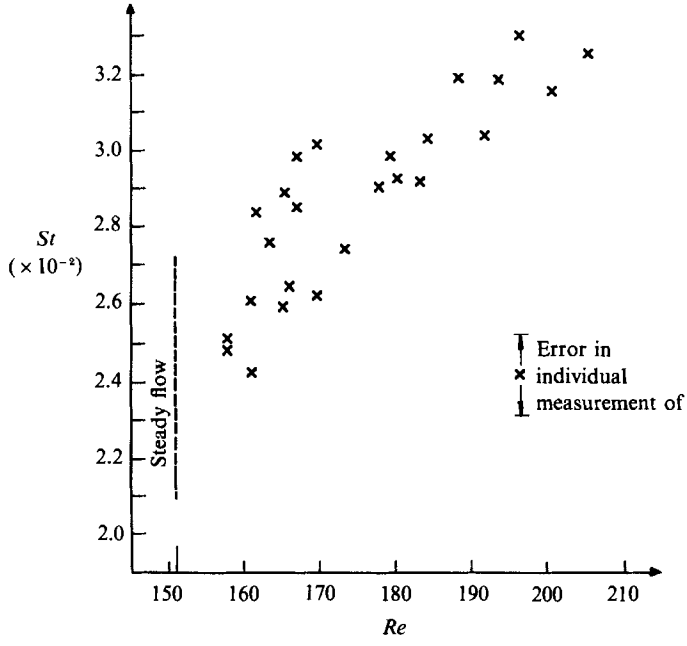

FIGURE 12. Variation of Strouhal number, St, with Reynolds number. $St = fd/U_0$ where f is the frequency, d the half-height of the upstream channel and U_0 the maximum inlet velocity.

numerical and experimental data and shows that the flow has recovered its parabolic profile by a downstream distance of 40 step-heights. A streamline plot of the flow at this Reynolds number is shown in figure 11.

This third separation region grew in length as Re was increased further up to a value of approximately 155, when the flow was observed to become unsteady. The time-dependence was characterized by the shedding of vortices, similar to those observed by Cherdron *et al.* (1978). These structures were shed almost periodically from the shear layer at the downstream end of the third recirculation. The amplitude of the flow oscillations was observed to increase for higher Reynolds number flows and the position of shedding was seen to move upstream along the shear layer of the third circulation. At higher Reynolds numbers still, the position of shedding changed to the tail of the long circulation region behind the step.

LDV measurements were used to investigate the initial onset of time-dependence. Power spectra were obtained by averaging sampled records over many periods of oscillation. The variation of the predominant frequency of oscillation f with Re, is shown in figure 12. The highest value of Re at which the flow remained steady was $Re = 151$. Above this critical value, the predominant frequency of oscillation rose almost linearly with Reynolds number from 0.8 ± 0.1 Hz at $Re = 154 \pm 1$ up to the maximum measured value of 1.7 ± 0.1 Hz at $Re = 207 \pm 1$. Variation of the measurement location within the flow was observed to have no effect on these results.

Data could be obtained wherever the fluctuation level was sufficient to permit recognizable spectra to be measured.

It was postulated that the flow initially became unsteady via a two-dimensional Hopf bifurcation of the solutions to the two-dimensional Navier–Stokes equations. Calculations were performed that searched for Hopf bifurcation, along the asymmetric solution branches, which correspond to Reynolds numbers close to the experimentally observed onset of time-dependence, using a technique described in Jackson (1987). Evidence suggested, however, that the loss of stability of the steady asymmetric flows to time-dependent ones did not occur via two-dimensional Hopf bifurcation in a channel of this configuration. Instead it seemed more likely that the observed unsteady flows were a consequence of three-dimensional effects in the channel.

The three-dimensional features of the flow were thus investigated by illuminating the flow in planes parallel to the bottom and top walls of the channel. Observations showed that the flow remained two-dimensional across the width of the channel, except for thin boundary layers close to the channel sidewalls, for Reynolds numbers up to approximately 140. These results support the evidence of figures 3–11, that the flow is nominally two-dimensional in the Reynolds number range where the flow first becomes asymmetric.

Three-dimensional circulations were distinct, however, in an apparently steady flow, with a Reynolds number of 140. Thus the flow in this configuration became three-dimensional before it became unsteady. Evidence thus suggests that the observed time-dependence may be caused by a three-dimensional disturbance. A more detailed description of the three-dimensional and time-dependent effects may be found in Fearn (1988).

5. Conclusions

The sequence of events reported here is similar to those described in other experimental studies of flows in a plane, symmetric two-dimensional channel expansion. An explanation of the observed steady asymmetric flows which occur has, however, been afforded by use of ideas from bifurcation theory. In particular, close agreement between experimental and numerical results have highlighted the occurrence of symmetry-breaking bifurcation. The subsequent steady asymmetric flows have been shown to be solutions of the two-dimensional Navier–Stokes equations.

Numerical calculations have shown that the observed time-dependent flows do not arise at a two-dimensional Hopf bifurcation. Thus the mechanism that can lead to time-dependence and chaos in the Taylor–Couette closed system, described by Mullin & Cliffe (1986), does not appear to carry over to time-dependent flows in this open system. Instead, experimental evidence suggests that three-dimensional effects may be significant in the development of these unsteady flows.

We hope to extend the investigation reported here to increase our understanding of the process by which the flow proceeds to turbulence. The experimental results of this future study will be analysed with recently developed signal processing techniques (Broomhead & King 1986). This knowledge may then be used in the application of flows in this particular geometry to areas of engineering interest. These include the usage of such flows as logical, bi-stable (flip-flop) devices, or in combustion processes, where a sudden expansion is used to create a recirculation zone which behaves as a flameholder.

Finally, the ideas developed and the conclusions reached from this study may lead to a fuller understanding of the development of other open channel flows in which bifurcation and non-uniqueness are observed to occur.

The research of R.M.F. was supported by an SERC CASE studentship with Harwell Laboratory, T.M. by the SERC Nonlinear Initiative and K.A.C. by the Underlying Research Programme of the UKAEA and by the Royal Society under the Royal Society/SERC Industrial Fellowship scheme.

REFERENCES

ABBOTT, D. E. & KLINE, S. J. 1962 Experimental investigations of subsonic turbulent flow over single and double backward-facing steps. *Trans. ASME* D: *J. Basic Engng* **84**, 317

BROOMHEAD, D. S. & KING, G. P. 1986 Extracting qualitative dynamics from experimental data. *Physica* **20D**, 217.

CHERDRON, W., DURST, F. & WHITELAW, J. H. 1978 Asymmetric flows and instabilities in symmetric ducts with sudden expansions. *J. Fluid Mech.* **84**, 13.

CLIFFE, K. A. 1989 Numerical calculations of symmetry-breaking in a two-dimensional channel. In preparation.

CLIFFE, K. A. & GREENFIELD, A. C. 1982 Some comments on laminar flow in symmetric two-dimensional channels. *Harwell Rep.* AERE-TP 939.

DRAZIN, P. G. & REID, W. H. 1982 *Hydrodynamic Stability*. Cambridge University Press.

DURST, F., MELLING, A. & WHITELAW, J. H. 1974 Low Reynolds number flow over a plane symmetrical sudden expansion. *J. Fluid Mech.* **64**, 111.

FEARN, R. M. 1988 Bifurcation of the flow in a sudden symmetric expansion. D. Phil. thesis, University of Oxford.

FUCHS, L. 1988 Incompressible vortex flows: non-uniqueness and hysteresis. In *Proc. Intl. Conf. on Numerical Methods in Fluid Dynamics*.

JACKSON, C. P. 1987 A finite-element study of the onset of vortex shedding in the flow past variously shaped bodies. *J. Fluid Mech.* **182**, 23.

JOHN, P. 1984 Plane sudden expansion flows and their stability. Ph.D. thesis, University of London.

MULLIN, T. & CLIFFE, K. A. 1986 Symmetry-breaking and the onset of time dependence in fluid mechanical systems. In *Nonlinear Phenomena and Chaos* (ed. S. Sarkar), pp. 96–112. Adam Hilger.

PFISTER, G., SCHMIDT, H., CLIFFE, K. A. & MULLIN, T. 1988 Bifurcation phenomena in Taylor–Couette flow in a very short annulus. *J. Fluid Mech.* **191**, 1.

REVISTO, A. & WHITELAW, J. H. 1978 Turbulence characteristics of the flow downstream of a symmetric, plane sudden expansion. *Trans. ASMEI*: *J. Fluids Engng.* **100**, 308.

SOBEY, I. J. 1985 Observation of waves during oscillatory channel flow. *J. Fluid Mech.* **151**, 395.

SOBEY, I. J. & DRAZIN, P. G. 1986 Bifurcations of two-dimensional channel flows. *J. Fluid Mech.* **171**, 263.